ISSN 1674-1056
http://cpb.iphy.ac.cn
http://iopscience.iop.org/cpb
中国物理 B
Chinese Physics
中国物理
Chinese Physics B

Optimization of pick-up coils for weakly damped SQUID gradiometers

Kang Yang(杨康), Jialei Wang(王佳磊), Xiangyan Kong(孔祥燕), Ruihu Yang(杨瑞虎), Hua Chen(陈桦)
Citation: Chin. Phys. B . 2018, 27(5): 050701. **doi:** 10.1088/1674-1056/27/5/050701

Journal homepage: http://cpb.iphy.ac.cn; http://iopscience.iop.org/cpb

What follows is a list of articles you may be interested in

Performance study of aluminum shielded room for ultra-low-field magnetic resonance imaging based on SQUID: Simulations and experiments

Bo Li(李波), Hui Dong(董慧), Xiao-Lei Huang(黄小磊), Yang Qiu(邱阳), Quan Tao(陶泉), Jian-Ming Zhu(朱建明)
Chin. Phys. B . 2018, 27(2): 020701. **doi:** 10.1088/1674-1056/27/2/020701

A dual-axis, high-sensitivity atomic magnetometer

Rujie Li(李茹杰), Wei Quan(全伟), Wenfeng Fan(范文峰), Li Xing(邢力), Zhuo Wang(王卓), Yueyang Zhai(翟跃阳), Jiancheng Fang(房建成)
Chin. Phys. B . 2017, 26(12): 120702. **doi:** 10.1088/1674-1056/26/12/120702

Indirect pumping bell-bloom magnetometer

Meng-Bing Wang(王梦冰), Da-Fa Zhao(赵大法), Gui-Ying Zhang(张桂迎), Kai-Feng Zhao(赵凯锋)
Chin. Phys. B . 2017, 26(10): 100701. **doi:** 10.1088/1674-1056/26/10/100701

Spin dynamics of magnetic resonance with parametric modulation in a potassium vapor cell

Rui Zhang(张锐), Zhi-Guo Wang(汪之国), Xiang Peng(彭翔), Wen-Hao Li(黎文浩), Song-Jian Li(李松健), Hong Guo(郭弘)
Chin. Phys. B . 2017, 26(3): 030701. **doi:** 10.1088/1674-1056/26/3/030701

Digital coherent detection research on Brillouin optical time domain reflectometry with simplex pulse codes

Hao Yun-Qi, Ye Qing, Pan Zheng-Qing, Cai Hai-Wen, Qu Rong-Hui
Chin. Phys. B . 2014, 23(11): 110703. **doi:** 10.1088/1674-1056/23/11/110703

Optimization of pick-up coils for weakly damped SQUID gradiometers*

Kang Yang(杨康)[1,2,3], Jialei Wang(王佳磊)[1,2,3], Xiangyan Kong(孔祥燕)[1,2,3,†], Ruihu Yang(杨瑞虎)[1,2,3], and Hua Chen(陈桦)[1,2,3]

[1] State Key Laboratory of Functional Materials for Informatics, Shanghai Institute of Microsystem and Information Technology (SIMIT), Chinese Academy of Sciences (CAS), Shanghai 200050, China

[2] CAS Center for Excellence in Superconducting Electronics (CENSE), Shanghai 200050, China

[3] University of Chinese Academy of Sciences, Beijing 100049, China

(Received 25 December 2017; revised manuscript received 2 March 2018; published online 26 April 2018)

The performance of a superconducting quantum interference device (SQUID) gradiometer is always determined by its pick-up coil geometry, such as baseline and radius. In this paper, based on the expressions for the coupled flux threading a magnetometer obtained by Wikswo, we studied how the gradiometer performance parameters, including the current dipole sensitivity, spatial resolution and signal-to-noise ratio (SNR), are affected by its pick-up coil via MatLab simulation. Depending on the simulation results, the optimal pick-up coil design region for a certain gradiometer can be obtained. To verify the simulation results, we designed and fabricated several first-order gradiometers based on the weakly damped SQUID with different pick-up coils by applying superconducting connection. The experimental measurements were conducted on a simple current dipole in a magnetically shielding room. The measurement results are well in coincidence with the simulation ones, indicating that the simulation model is useful in specific pick-up coil design.

Keywords: superconducting quantum interference device (SQUID) gradiometer, spatial resolution, dipole sensitivity, signal-to-noise ratio

PACS: 07.55.Ge, 85.25.Am, 85.25.Dq, 87.55.de **DOI:** 10.1088/1674-1056/27/5/050701

1. Introduction

Superconducting quantum interference devices (SQUIDs) are widely used in weak biomagnetic signal detection, such as magnetocardiography (MCG) and magnetoencephalography (MEG), due to their high magnetic field sensitivity.[1–3] Usually, it is a challenge to extract MCG or MEG signals from extremely high environmental magnetic noise whose intensity can reach up to several hundred micro-Tesla (μT). In order to restrain environmental noise and acquire high-quality biomagnetic signals for accurate diagnosis, magnetically shielding rooms (MSRs) built using aluminum and mu-metal alloy are always adopted. However, the MSR costs are considerably high to obtain a good shielding performance. To solve this problem, it is more practical to use SQUID gradiometers in a simple MSR, or even in an unshielded environment.[4–6]

A gradiometer always consists of a SQUID and a gradiometric pick-up coil, which can suppress background fields from distant sources while retaining substantially high sensitivity to nearby sources. A gradiometric coil is always formed by two or more coils which are coaxially connected in series but set in opposite directions. The performance of a gradiometer, usually the signal-to-noise ratio (SNR), is well studied depending on the baseline, i.e., the distance between the connected coils.[7,8] However, this evaluation is incomplete for a practical gradiometer. On the one hand, the performance of a gradiometer is not only related to the baseline but also depends on many other parameters, for example, the radius of the pick-up coil, the distance to the signal sources, and the order. On the other hand, the performance parameters including the spatial resolution and sensitivity are also essential for a gradiometer applied to clinic, such as accurate positioning and imaging.

In order to assess how the pick-up coil geometry affects the gradiometer performance parameters, many gradiometers with various baselines, radii, and orders should be fabricated and tested with a certain signal source in different spatial positions, which is too costly to execute. In this paper, based on the results obtained by Wikswo,[9] we present a model for the pick-up coil by numerical calculation. Focusing on the current dipole source, the relationships between the pick-up coil geometry and the spatial resolution, dipole sensitivity, and SNR of a SQUID gradiometer are well studied. Furthermore, depending on the weakly damped SQUID and superconducting connection we have developed,[10] several kinds of wire-wound axial first-order gradiometers with different baselines and radiuses are fabricated to verify the reliability of our simulation results.

*Project supported by the Key Project of Shanghai Zhangjiang National Innovation Demonstration Zone of the Special Development Fund, China (Grant No. 2015-JD-C104-060) and the National Natural Science Foundation of China (Grant No. 61741122).

†Corresponding author. E-mail: xykong@mail.sim.ac.cn

© 2018 Chinese Physical Society and IOP Publishing Ltd

2. Gradiometer simulation theory

In MEG or MCG studies, the current dipole is widely used as a mathematical model to describe the bioelectric currents. Here, we consider a dipolar current source $\boldsymbol{P}(p_x, p_y, 0)$ located at $(x', 0, z')$ and a pick-up coil centered on the z-axis in a Cartesian coordinate system (see Fig. 1). For simplicity, the analysis is based on the first-order gradiometer, which does not lose generality.

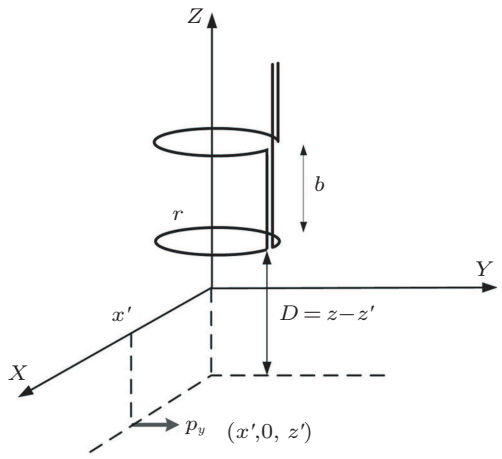


Fig. 1. Schematic of pickup coil of the first-order gradiometer. A current dipole source is placed at point $(x', 0, z')$. The vertical distance between the sensing loop of the pick-up coil and the dipole source is $D = z - z'$.

2.1. Signal-to-noise ratio

In order to simulate the SNR of a gradiometer, the output flux corresponding to a current dipole source detected by the pick-up coil should first be calculated. According to the derived results of Wikswo[9] for the flux threading a magnetometer, the flux through the pick-up coil of a first-order gradiometer is

$$\begin{aligned}\Phi_{\mathrm{g}} &= \frac{\mu_0 p_y}{k_1 \pi}\sqrt{\frac{r}{x'}}\left[\left(1-\frac{k_1^2}{2}\right)K(k_1)-E(k_1)\right] \\ &\quad + \frac{\mu_0 p_y}{k_2 \pi}\sqrt{\frac{r}{x'}}\left[\left(1-\frac{k_2^2}{2}\right)K(k_2)-E(k_2)\right], \end{aligned} \tag{1}$$

where

$$k_1^2 = \frac{4x'r}{[(x'+r)^2+(z-z')^2]}, \tag{2}$$

$$k_2^2 = \frac{4x'r}{[(x'+r)^2+(z-z'+b)^2]}, \tag{3}$$

$$K(k_i) = \int_0^{\frac{\pi}{2}} \frac{\mathrm{d}\varphi}{\sqrt{1-k_i^2\sin^2\varphi}}, \qquad i = 1, 2, \tag{4}$$

$$E(k_i) = \int_0^{\frac{\pi}{2}} \sqrt{1-k_i^2\sin^2\varphi}\,\mathrm{d}\varphi, \qquad i = 1, 2. \tag{5}$$

Here μ_0 is the vacuum permeability, b is the baseline, r is the radius of the pick-up coil and $D = z - z'$ is the vertical distance between the sensing loop of the pick-up coil and the dipole source. Note that p_x does not contribute to the overall flux for symmetry reasons.

The total flux noise (Φ_{n}) in the first-order gradiometer can be divided into two parts. One is the intrinsic noise Φ_{in}, which depends on the SQUID flux noise Φ_{SQ} and the mismatching between the input coil and the pick-up coil in the flux-transformer circuit Φ_{mis}. The other is the environmental noise Φ_{en}, which depends on the uniform magnetic field B_{u}, the magnetic field gradient G_1, and the balance level δ_{u}. The total flux noise can be expressed as

$$\Phi_{\mathrm{n}} = \sqrt{\Phi_{\mathrm{in}}^2 + \Phi_{\mathrm{en}}^2} \tag{6}$$

$$= \sqrt{\Phi_{\mathrm{SQ}}^2 + \Phi_{\mathrm{mis}}^2 + \Phi_{\mathrm{en}}^2} \tag{7}$$

$$= \sqrt{\frac{(L_{\mathrm{p}} + L_{\mathrm{in}})^4}{M_{\mathrm{i}}^4}\Phi_{\mathrm{SQ}}^2 + (B_{\mathrm{u}}\delta_{\mathrm{u}}A + G_1 bA)^2}. \tag{8}$$

Here A is the area of the pick-up coil, L_{p} and L_{in} are the inductances of the pick-up coil and the input coil, respectively, and M_{i} is the mutual inductance between the input coil and the SQUID loop. The parasitic inductance in the leads connecting the pickup coil and input coil is neglected. Then the SNR is given by

$$\mathrm{SNR} = 20\log\frac{\Phi_{\mathrm{g}}}{\Phi_{\mathrm{n}}}. \tag{9}$$

2.2. Current dipole sensitivity

The current dipole sensitivity refers to the minimum dipole that can be detected by a gradiometer. According to Eqs. (1)–(5), for a pick-up coil with certain baseline b, radius r and distance to the signal source D, the maximum flux can be obtained at the point $x'_{\max}$. If the maximum flux is equal to the SQUID flux noise Φ_{SQ}, the minimum detectable current dipole $p_{y\min}$ can be found at $x'_{\max}$, because in the position $x'_{\max}$, a small current dipole can lead to a larger flux rather than that at any other positions. So $p_{y\min}$ can be calculated as

$$\begin{aligned} p_{y\min} &= \frac{\pi\Phi_{\mathrm{SQ}}}{\mu_0}\left(\frac{r}{x'_{\max}}\right)^{-1/2}\left\{\left[\frac{1}{k_{1\max}} - \frac{k_{1\max}^2}{2}K(k_{1\max})\right.\right. \\ &\quad \left. - \frac{1}{k_{1\max}}E(k_{1\max})\right] - \left[\frac{1}{k_{2\max}} - \frac{k_{2\max}^2}{2}K(k_{2\max})\right. \\ &\quad \left.\left. - \frac{1}{k_{2\max}}E(k_{2\max})\right]\right\}^{-1}. \end{aligned} \tag{10}$$

Here, $k_{1\max}$ and $k_{2\max}$ are derived from Eqs. (2) and (3) by replacing x' with $x'_{\max}$, respectively.

2.3. Spatial resolution

The spatial resolution can be defined as the minimum detectable displacement of a current dipole. If a dipole moves a displacement δ corresponding to a certain flux variation $\Delta\Phi_{\mathrm{g}}$, then we can calculate the resolution as follows:

$$\begin{aligned}\Delta\Phi_{\mathrm{g}} &= \Phi_{\mathrm{g}}(x'+\delta) - \Phi_{\mathrm{g}}(x') \\ &= \Phi_{\mathrm{g}}(x') + \Phi'_{\mathrm{g}}(x')\delta + \frac{1}{2}\Phi''_{\mathrm{g}}(x')\delta^2 - \Phi_{\mathrm{g}}(x')\end{aligned}$$

$$= \Phi_g'(x')\delta + \frac{1}{2}\Phi_g''(x')\delta^2. \quad (11)$$

Here, $\Phi_g(x'+\delta)$ is expanded in a Taylor series of δ ($r \gg \delta$). At the point $x' = x'_{max}$, the condition $\Phi_g'(x'_{max}) = 0$ can be used to simplify Eq. (11). If we assume $\Delta\Phi_g = \Phi_{SQ}$, then the spatial resolution can be expressed as

$$\delta = \sqrt{\frac{2\Phi_{SQ}}{\Phi_g''(x'_{max})}}. \quad (12)$$

From Eqs. (10) and (12), it is obvious that the point x'_{max} corresponding to the maximum flux is important in our simulation. To determine x'_{max}, the maximum index function of MatLab should be used, because the analytical solution cannot be figured out due to the complexity of these formulas.

3. Gradiometer simulation results

In this part, we study the effect of the geometry parameters b, r and the position parameter z' on the above three performance parameters. Note that the position parameter x' is set to x'_{max}, because the optimal performance is obtained here for a current dipole as we have discussed before. To reduce the involved variables, we introduce the dimensionless quantities normalized by $D = z - z'$, i.e., $R = r/D$ and $B = b/D$ to replace r and b in Eqs. (1)–(5), and the simulation is based on the numerical calculation by MatLab. Here, the ranges of R and B are respectively set to be $(0,5)$ and $(0,10)$ during the simulation, which is enough and practical after considering the MCG system inner space and the gradiometer fabricating cost.

When discussing the SNR of a gradiometer, the characters of the dipole source should be defined, as the flux output is also affected by the intensity and the position of the source. Here, we assume $p_y = 10$ pA·m and $D = 15$ mm for a typical situation. Figure 2 shows the actual SNR curves as a function of the baseline and radius. Here, the gradient balance level is assumed to be 10^{-3}, the uniform magnetic field B_u and the magnetic field gradient G_1 are set as 4 nT and 45 nT/m, which are measured in our MSR. The results show the strong dependence of the SNR on B and R of the pick-up coil, which can be further confirmed by the projected curves ($B = 5$, $R = 1$) on the XZ and YZ planes. On the one hand, a larger radius of the pick-up coil means more flux coupled into the SQUID, resulting in an increasing SNR ($R = 1$ to 3, when $B = 5$). However, the decreasing line ($R > 3$) indicates that a large radius cannot unlimitedly increase the SNR, because the flux noise also increases due to the mismatching between the input coil and the pick-up coil and the increase of the environmental noise. On the other hand, the relationship between the SNR and baseline with a certain radius (such as $R = 1$) presents a similar tendency trend, which means that an optimal baseline exists to obtain a high SNR.

Figure 3 plots the dipole sensitivity as a function of the normalized radius R and baseline B. The minimum detectable current dipole is normalized by $\pi\Phi_{SQ}/\mu_0$ for generality consideration. Here, a small value of $\mu_0 p_y/(\pi\Phi_{SQ})$ implies a high sensitivity. For a certain baseline, such as $B = 5$, the sensitivity improves rapidly when the increasing R is smaller than 1, and it improves slowly when $R > 1$. Theoretically, the sensitivity can improve without limits by increasing the radius, but it is not practical. Furthermore, increasing B cannot always lead to a higher sensitivity (parallel curves of $B = 6$–10), because the gradiometer performs more like a magnetometer in these cases, which is more obvious in the YZ plane when $R = 1$.

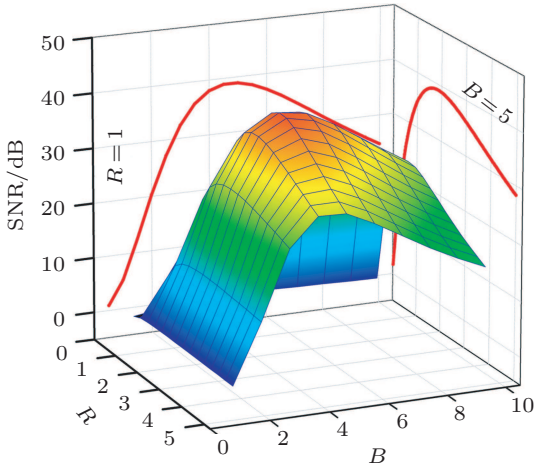


Fig. 2. (color online) The SNR simulation result as a function of radius r and baseline b. Here, R and B are dimensionless quantities divided by constant $D = 15$ mm for uniformity consideration. The curve projected on the XZ plane represents the relationship between SNR and R when B is set to 5. And the curve on the YZ plane shows how B affects the SNR when $R = 1$.

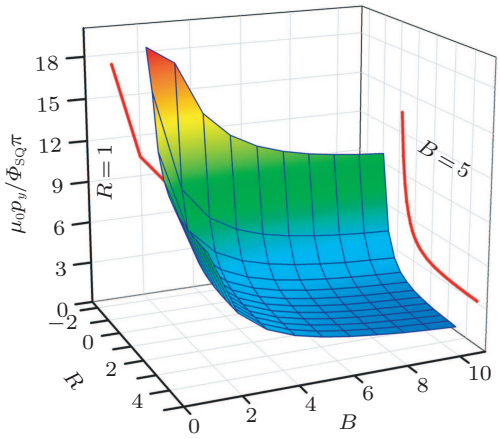


Fig. 3. (color online) Normalized dipole sensitivity plotted as a function of the gradiometer baseline and radius. The curves projected on the XZ and YZ planes show the detail.

Figure 4 shows the spatial resolution normalized by $\frac{1}{D}\sqrt{\frac{\mu_0 p_y}{\pi\Phi_{SQ}}}$ as a function of R and B. The smaller the value of $\frac{\delta}{D}\sqrt{\frac{\mu_0 p_y}{\pi\Phi_{SQ}}}$, the higher the spatial resolution. For very small pick-up coils or distant current dipoles ($R \to 0$), the sensitivity deteriorates because the dipole have to move a large distance

to reach the settled flux variation Φ_{SQ}. For large pick-up coils and close current dipoles ($R \to 5$), the resolution hardly improves. The long baselines ($B = 6$–10) do not significantly improve the spatial resolution either, which is shown in the dark blue flat area.

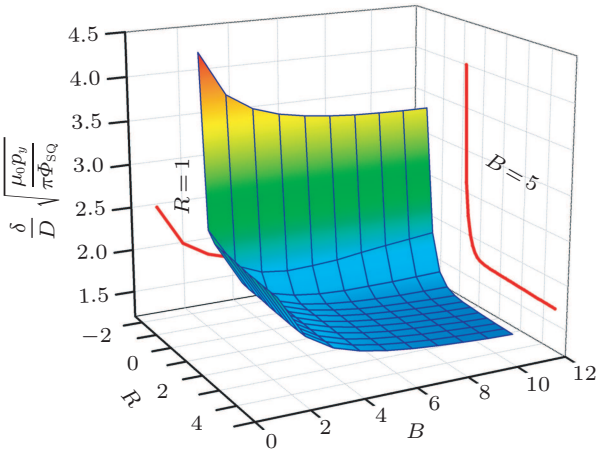


Fig. 4. (color online) Normalized spatial resolution as a function of the gradiometer baseline and radius. The curves of $R = 1$ and $B = 5$ show how the baseline and radius affect the resolution.

The simulation results not only indicate the dependence of the three parameters on the baseline and radius, but also are useful in determining the geometry design region of the pick-up coil of a practical first-order gradiometer (see Fig. 5). For example, if we consider a source ($p_y = 10$ pA·m) located at 15 mm away from the gradiometer in an MSR ($B_u = 4$ nT, $G_1 = 45$ nT/m), the gradiometer balance level is assumed to be 10^{-3}, and the SQUID noise is 60 $\mu\Phi_0$ in the 100 Hz bandwidth. Here, we set the influencing factors as typical constants which are measured in our real system, and the electronic noise is converted into SQUID noise. Then, for a target SNR of 36 dB, the reasonable range of the baseline is from 57 mm to 97.5 mm, and the radius should be set from 22.5 mm to 48 mm. Then considering the sensitivity superior to 1.0 pA·m, the optimal baseline and radius should be larger than 30 mm and 69.5 mm, respectively. If the spatial resolution of interest is smaller than 0.3 mm, then the optimal baseline and radius would be larger than 30 mm and 75 mm, respectively. Finally, the applicable ranges of the baseline (69.5 mm to 97.5 mm) and the radius (30 mm to 48 mm) can be figured out by intersecting all the ranges. Considering the system inner space, it is usual to choose the minimum applicable baseline and radius, i.e., $b = 69.5$ mm and $r = 30$ mm, and the corresponding inductance of the pick-up coil is 452.6 nH.

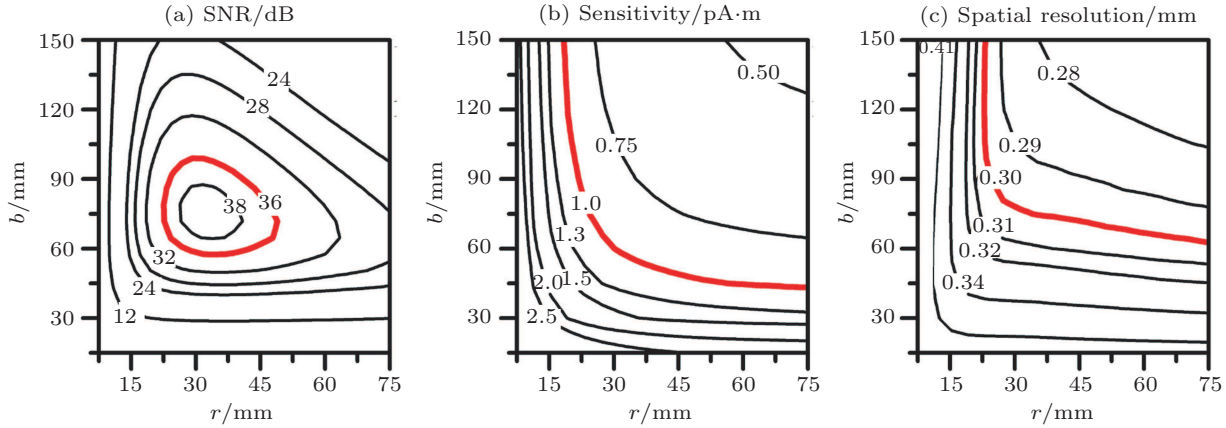


Fig. 5. (color online) Isograms of three performance parameters plotted as a function of the radius and baseline. (a) SNR curve, the red line represents SNR = 36. (b) Sensitivity curve, the red line represents sensitivity equal to 1.0 pA·m. (c) Spatial resolution curve, the red line represents resolution equal to 0.3 mm. Here, $D = 15$ mm, $p_y = 10$ pA·m, $B_u = 4$ nT, $G_1 = 45$ nT/m, $\Phi_{SQ} = 60$ $\mu\Phi_0$, and $\delta_u = 10^{-3}$.

4. Experimental setup and results

The SQUID used to verify the simulation results is based on weakly damped Josephson junctions with large Stewart–McCumber parameter $\beta_c \approx 5$. By setting the shunt resistance to 33 Ω, a large flux-to-voltage transfer coefficient can be obtained to suppress the preamplifier noise.[11] Figure 6(a) shows the design layout with chip size of 5 mm×3 mm. Here, the feedback coil is rearranged in the flux-transformer circuit, which functions in external feedback mode, to eliminate the crosstalk in the multi-channel system.[12] The inductance of the secondary coil in the flux-transformer circuit which is coupled to the feedback coil is 10 nH, and that of the input coil is 220 nH. In simulation, the inductance of the input coil is considered to be 230 nH because these two coils are connected in series. The axial pick-up coil is formed by two single-turn coils, a sensing coil and a compensation coil. These two coils are made by Nb superconducting wires and wound in opposite directions coaxially on a reinforced fiberglass epoxy rod. The pick-up coil and the SQUID chip are set in the slot of the processed rod. The superconducting connection is essential here. On the one hand, it can reduce the distance between the SQUID chip and the pickup coil and increase the working duration of the gradiometer. On the other hand, the SQUID flux noise should be a constant during the measurement. However, we only picked out four satisfying chips with the same noise

performance of 5 $\mu\Phi_0/\sqrt{\text{Hz}}$. The superconducting connection can ensure the nondestructive bonding between one SQUID chip and several pickup coils to make different gradiometers. It is impossible to verify all the simulated points, and several first-order gradiometers with different baselines ($b = 50$ mm, 70 mm) and radii ($r = 5$ mm, 7.5 mm, 10 mm, 12.5 mm) have been fabricated and installed in the four-channel verification system.

The system is operated inside an MSR. Four gradiometers with the same baseline are mounted on the bottom of a non-magnetic cryostat each time, and the distance between the sensing coil and the outer bottom of the cryostat is kept at 13 mm. Signals can be read out by direct readout electronics and sampled with a 24-bit A/D card at a sampling rate of 1 kHz. A step control platform with a high precision of 0.1 mm is placed 30 cm under the cryostat, which can be controlled by a driver to move along the XY direction. A current dipole with an adjustable intensity ranging from 1 pA·m to 1 nA·m is fixed on the platform, 2 mm apart from the outer bottom of the cryostat. It is worth noting that the least squares algorithm is used here to suppress the magnetic noise introduced by the platform. And the frequency of the excitation signal is chosen to be 86 Hz to avoid low-frequency and power frequency interference.

Figure 7 shows the measured and the simulated performance parameters of the first-order gradiometer. The black and red lines respectively represent the simulation results as a function of the radius with two different baselines ($b = 50$ mm, 70 mm), deriving from the 3D graphs we discussed above by introducing the distance ($D = 15$ mm) and the actual SQUID parameters into the normalized variables. The black and red dots show the measured performance parameters with these two baselines. As can be seen from Figs. 7(a) and 7(b), the measured SNR and sensitivity are deviated from the simulated ones by 10.3% ($b = 50$ mm) and 11.1% ($b = 70$ mm) on average, which indicates that some other unexpected environmental noises exist. Also, the systematic error and the circuit noise from the control and data acquisition units inevitably contribute to the deviation. Expect for the measuring discrepancy, figure 7(c) shows the overlapping resolution dots

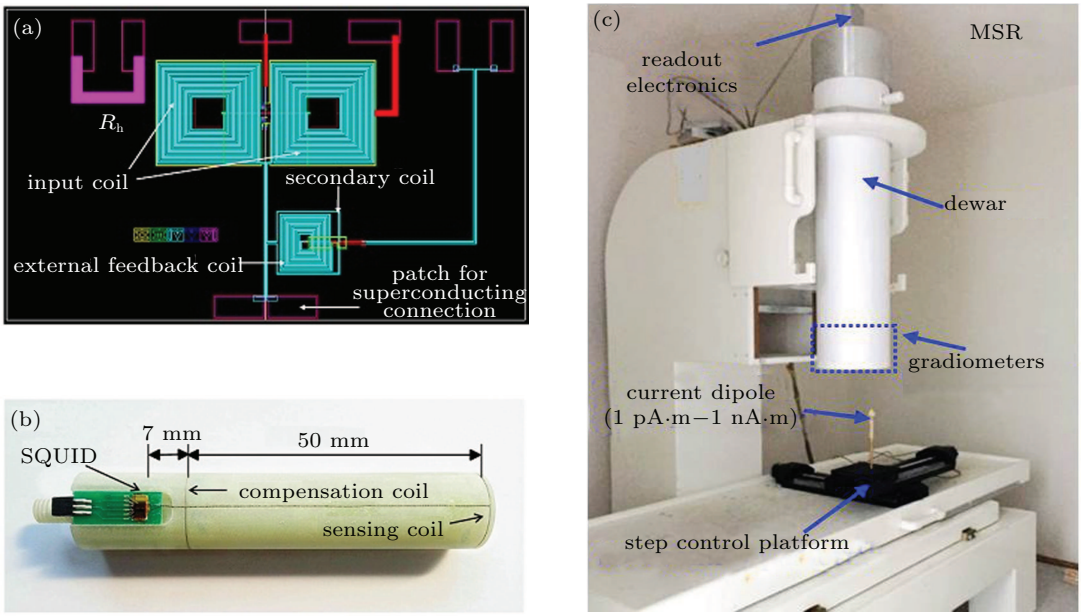


Fig. 6. (color online) (a) Layout of the SQUID. (b) The first-order gradiometer with baseline of 50 mm. (c) Four-channel verification system in MSR.

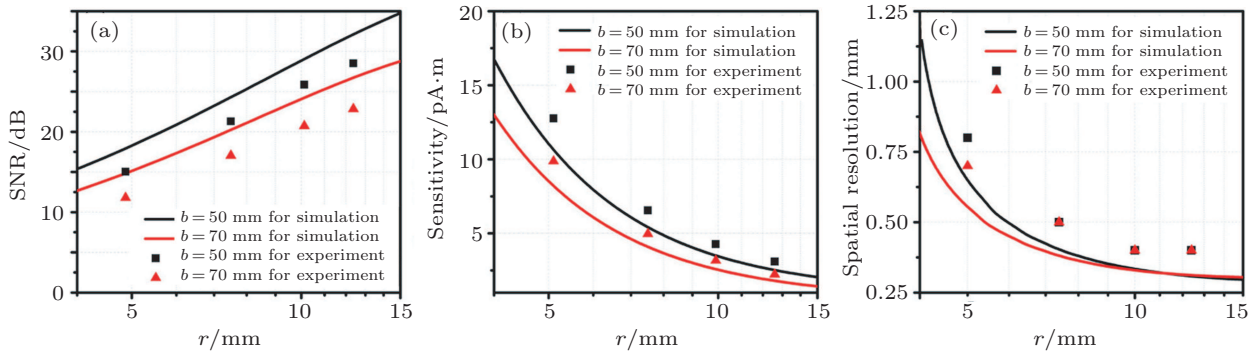


Fig. 7. (color online) Simulated and measured results of (a) SNR, (b) sensitivity, and (c) spatial resolution. The black and red solid lines are the simulated results for $b = 50$ mm and $b = 70$ mm, respectively. The dots with the same color represent the corresponding measured results.

($r = 7.5$ mm, 10 mm, 12.5 mm), which is caused by the precision limit of the step platform. However, when $b = 50$ mm, the correlation coefficients between the simulated results and the measured results of SNR, sensitivity, and spatial resolution are 93.7%, 95.4%, and 92.1%, respectively, and the coefficients are 93.5%, 95.2%, and 90.4% when $b = 70$ mm, indicating the effectiveness of the pick-up coil model.

5. Conclusion

We investigate how pick-up coil geometry can affect gradiometer performance. The SNR, dipole sensitivit, and spatial resolution are considered as three important performance parameters. Based on Wikswo's result, a numerical model for the first-order pick-up coil has been proposed and simulated. Both the SNR and spatial resolution are limited by the baseline and radius because over-sized pickup coils can result in mismatching with the input coil in the flux-transformer circuit. Theoretically, any high sensitivity can be reached by increasing the radius without practical consideration. The simulation results can be applied to determine a reasonable region for the pick-up coil design by setting target performance parameter in the isogram. Furthermore, first-order gradiometers based on a weakly damped DC SQUID in external feedback mode have been fabricated and a four-channel system has been built to verify the simulation results in certain cases. It turns out that the correspondence between the simulation and measurement is satisfactory, indicating the reliability of the gradiometer model. Such a model is also effective in analyzing high-order gradiometers and will be used for gradiometer design in our multichannel MCG system in the future.

References

[1] Liu C, Zhang Y, Muck M, Zhang S L, Krause H J, Braginski A I, Zhang G F, Wang Y L, Kong X Y, Xie X M, Offeharsser A and Jiang M H 2013 *Supercond. Sci. Technol.* **26** 065002

[2] Lee Y H, Kwon H C, Kim J M, Park Y K and Park J C 1999 *IEEE Trans. Magn.* **35** 4097

[3] Kong X Y, Zhang Y, Xie X M and Jiang M H 2013 *IEICE Trans. Electron.* **E96-C** 320

[4] Lee Y H, Yu K K, Kim J M, Kwon H, Kim K and Park Y K 2008 *Physica C* **468** 1942

[5] Kang C S, Lee Y H, Yu K K, Kwon H, Kim J M, Kim K, Lim H K, Park Y K and Lee S G 2009 *IEEE Trans. Magn.* **45** 2882

[6] Kong X Y, Zhang S L, Wang Y L, Zeng J and Xie X M 2012 *Phys. Procedia* **36** 286

[7] Alexander G 1999 *IEEE Trans. Appl. Supercond.* **9** 3676

[8] Li H, Zhang S L, Qiu Y, Zhang Y S, Zhang C X, Kong X Y and Xie X M 2015 *Chin. Phys. B* **24** 028501

[9] Wikswo J P 1978 *AIP Conf. Proc.* **44** p. 145

[10] Yang K, Chen H, Kong X Y, Lu L, Li M, Yang R H and Xie X M 2016 *IEEE Trans. Appl. Supercond.* **26** 1602205

[11] Zhang Y, Liu C, Schmelz M, Krause H J, Braginski A I, Stolz R, Xie X M, Meyer H G, Offenhausser A and Jiang M H 2012 *Supercond. Sci. Technol.* **25** 125007

[12] Brake H J M, Fleuren F H, Ulfman J A and Flokstra J 1986 *Cryogenics* **26** 667